MANCHESTER 1824
The University of Manchester

The University of Manchester Research

Wind Turbine Blade Bearing Fault Detection with Bayesian and Adaptive Kalman Augmented Lagrangian Algorithm

Link to publication record in Manchester Research Explorer

Citation for published version (APA):
Zhang, C., Liu, Z., & Zhang, L. (Accepted/In press). *Wind Turbine Blade Bearing Fault Detection with Bayesian and Adaptive Kalman Augmented Lagrangian Algorithm*.

Citing this paper
Please note that where the full-text provided on Manchester Research Explorer is the Author Accepted Manuscript or Proof version this may differ from the final Published version. If citing, it is advised that you check and use the publisher's definitive version.

General rights
Copyright and moral rights for the publications made accessible in the Research Explorer are retained by the authors and/or other copyright owners and it is a condition of accessing publications that users recognise and abide by the legal requirements associated with these rights.

Takedown policy
If you believe that this document breaches copyright please refer to the University of Manchester's Takedown Procedures [http://man.ac.uk/04Y6Bo] or contact uml.scholarlycommunications@manchester.ac.uk providing relevant details, so we can investigate your claim.

OPEN ACCESS

Download date:12. Nov. 2022

Wind Turbine Blade Bearing Fault Detection with Bayesian and Adaptive Kalman Augmented Lagrangian Algorithm

Chao Zhang[a], Zepeng Liu[b], Long Zhang[a,*]

[a] *Department of Electrical and Electronic Engineering, University of Manchester, UK*
[b] *Department of Automatic Control and Systems Engineering, University of Sheffield, UK*

Abstract

As a critically supporting and rotational component for wind turbines, blade bearings need special health monitoring for safe operation in actual industrial conditions. One of the main difficulties of the wind turbine blade bearing condition monitoring is noisy signals generated under fluctuating slow speed with heavy loads. This is because blade bearing rotation speed is influenced by blade flipping and external disturbances, and this influence is time-varying. This paper proposes a new method, Bayesian and Adapted Kalman Augmented Lagrangian (BAKAL), to filter the signal under this time-varying condition. The new method uses a two-step search (coarse and fine search) to deal with the filtering process based on Bayesian Augmented Lagrangian (BAL) framework. In addition, both linear and nonlinear effects and their sparsity are considered for model construction. Finally, the smearing problem in the frequency spectrum is dealt with through signal resample in the order domain for superior performance of fault diagnosis. The proposed BAKAL algorithm is strictly validated in several experiments under approximately fixed speed and variable speed within the condition of heavy loadings. The experiments use an industrial and rotational wind turbine blade bearing with natural defects, which has been served in an actual wind power plant for over 15 years. The experimental results demonstrate the effectiveness of the proposed method.

Keywords: Acoustic emission analysis, Time-varying system, Slow-speed system, Blade bearing fault diagnosis, Bayesian and Adapted Kalman Augmented Lagrangian (BAKAL), System identification

1. Introduction

Wind power, as efficient energy, is carbon emission-free and available everywhere in nature and has gradually grown into one of the most widespread renewable types of energy, with the form of clean energy [1]. The global statistical data about wind energy shows, the global total installed wind power capacity was only 23.9 GW in 2001, rising to 486.8 GW in 2016 and over 800 GW in 2021 [2].

The reliability of wind turbines in actual industrial operations is an issue because long-term exposure in harsh circumstances and mechanical wear will cause some damage to a wind turbine, and this will influence energy conversion efficiency, especially for an inner component such as wind turbine blade bearings [3, 4]. Some defects in wind turbine blade bearings may result in severe degradation of energy conversion efficiency [5], compared with healthy wind turbine blade bearings. Regular inspection by engineers of wind turbine blade bearings needs many human and material resources, which may be unreliable and costly. Therefore, it is essential to develop portable and efficient condition monitoring and fault diagnosis methods (CMFD) for wind turbine blade bearings to detect damage and defects to prevent enormous economic loss [6].

Through multifaceted considerations and comparisons among frequently-used sensors, such as optical sensors and vibration sensors, an acoustic emission (AE) sensor is adopted in this paper for its high sensitivity

*Corresponding Author
Email address: long.zhang@manchester.ac.uk (Long Zhang)

in the frequency [7] (range from 1 kHz to 1 MHz in this work). The high sensitivity of AE sensors means that as much weak and subtle information as possible can also be collected for comprehensive analysis. However, the high sensitivity of AE sensors may introduce some redundant and noisy components, resulting in contamination of the fault signal [8]. In addition, it is worth noting that more redundant and noisy components contribute to more accurate noise model construction in our proposed method, which can help extract fault signals better. Generally, the high sensitivity of an AE sensor is significant for the proposed method in this paper.

If a fault exists in a wind turbine blade bearing, the raw AE signal generally consists of two components: deterministic and fault signals. The deterministic signals are often undesired noise, such as mechanical rotation movements and electric signals, that has to be eliminated. Moreover, the fault signals generated due to damaged components are useful for further analysis, and it is highly desirable for them to be separated from the raw AE signals. After the fault signals have been extracted skilfully from the raw AE signal, the CMFD of large-scale wind turbine blade bearings benefits from pure fault signal to achieve better diagnosis results [9].

Many types of methods have been developed to filter signals. However, methods used to denoise signals from wind turbine blade bearings are limited. This is because large-scale wind turbine applications began 15 years ago, and damage generation usually occurs over ten years. In other words, it is a problem that was only recently discovered by the industry and was seldom researched before, so general bearing research studies are reviewed next.

Signal denoising methods are mainly classified as the statistical approach and modelling approach. For the statistical approach, Aye et al. [10] adopted the Principal Component Analysis (PCA) method to subtly detect damage to a bearing under variable slow-speed conditions. Guo et al. [11] utilized the matrix decomposition method, k-means singular value decomposition (K-SVD), for fault diagnosis of wind turbine bearings. The primary characteristics of these statistical approaches are that few assumptions and constraints are required for collected data. However, the ability to distinguish the fault signals and deterministic signals may not be satisfactory in some cases. For the modelling approach, Zhang et al. [12] proposed a type of ARMA-based method with reinforcement learning to construct a model for fault diagnosis. Yuan et al. [13] utilized series neural network LSTM to judge whether it is a faulty condition and to predict the remaining useful life. The modelling approach may obtain accurate and convincing results if all the constraints and feeding data are sufficient. However, the construction process of the model may not be easily implemented for limited data applications (For instance, the ARMA model often requires appropriate data distribution and the LSTM model often needs mass data input and general data cycle).

After analyzing the advantages and disadvantages of the statistical and modelling approaches, our paper mainly focuses on the modelling-based denoising approach to eliminate the deterministic signals from the raw AE signal. Before model construction, the maintenance conditions of wind turbine blade bearings have to be considered. Modern wind turbines have a maintenance detection state, and the blade bearing can rotate 360 degrees for maintenance in this state. The fault detection in this paper is not executed in an operative state but in a maintenance detection state. Wind turbines can enter the maintenance detection state at a fixed period, such as every month, to conduct a detailed and accurate check. The maintenance process consists of three phases (start, oscillation, stop). At the start phase, the blade rotation speed of a wind turbine increases its speed to a desired level, i.e., the ascending curve. In the oscillation phase, the rotation speed tracks the desired speed, but external factors (such as unbalanced loads) result in oscillating phenomena during this phase. During the stop phase, the rotation speed drops to zero speed, i.e., the descending curve. This paper focuses attention on the oscillation phase. Existing work Bayesian Augmented Lagrangian (BAL) [14] simplified the oscillation phase as a time-invariant one during model construction, utilizing a type of Lagrangian-based algorithm to separate the fault signals. The simplified system may deal with a simple and slow time-varying situation, but it does not fully use the collected raw signal during the oscillation phase for accurate model construction. In addition, unbalanced loads (including wind load, blade load, voltage load, etc.) result in an oscillation phase that is not a complete time-invariant state, so the performance of the time-invariant method can be limited if the oscillation is large or fast. To sum up, considering that the original BAL method only regards the oscillating phase as a time-invariant system, a valid time-varying model construction may be desirable for the oscillation phase to better extract the fault signals in collected

signals.

This paper focuses on the blade bearing fault detection under fluctuating slow speed with heavy loads, which is operated under maintenance periods. This paper mainly considers the time-varying factors in the oscillation phase. This solution is achieved by extending the existing BAL method to pursue fine-grained filtering performance. Furthermore, this paper improves parameter optimization process with two steps (coarse and fine search) to improve model parameter estimation during model construction. The coarse search is for the low-hierarchy parameter estimation without considering the relationship among all windows, and the fine search is the high-hierarchy parameter estimation that makes full use of Kalman filter to construct a bond for each window, contributing to filtering performance. Using two-step search techniques in the proposed Bayesian and Adapted Kalman Augmented Lagrangian (BAKAL) algorithm, the fault signal can be separated flexibly, and this reduces the difficulties in later frequency or order analysis for fault diagnosis. To rationally estimate the shape of deterministic signals in the raw AE signals and avoid drawbacks of linear methods such as discrete/random separation (DRS) [15], both linearity and non-linearity are considered in advance for model construction. The complexity of the nonlinear model due to the redundant linear or nonliterary terms is further reduced by sparse representation techniques [16, 17]. After separation of the fault signal, the 'smearing problem' in frequency spectrum is addressed through signal resample in order domain for superior fault diagnosis performance.

In essence, the major work of this paper can be summarized as follows:

1) A new method, BAKAL, is proposed to denoise the blade bearing signal under fluctuating slow speed, considering time-varying factors. The noise model parameter estimation is optimized with two step approaches with coarse and fine search in order to get optimized filtering performance. In addition to the two advantages mentioned above, the new BAKAL method also enjoys the advantages of the original BAL method, including the nonlinear approximation and sparse model representation.

2) Regarding the 'smearing problem' in the frequency spectrum, the denoised signal is resampled into the order domain to make the order analysis for accurate fault diagnosis.

3) This paper validates the proposed BAKAL algorithm at approximately fixed speed without a blade (Test 1) and fluctuating speed with a blade (Test 2 and Test 3), with an industrial-scale and naturally damaged wind turbine which has been operated in a real wind farm for over 15 years.

2. Prior Knowledge

2.1. Frequency or Order Domain Analysis

In order to find the defect frequency and determine the defect type, frequency or order domain analysis is required. The frequency or order domain analysis is a crucial step for fault diagnosis, which can transform the original signal in the time domain into an intuitive signal in the frequency or order domain so that the faults can be diagnosed easily. For the non-stationary signal with variable speed, it can be resampled by a constant angle increment. Therefore, the time domain non-stationary signal will be a stationary signal in the angle domain, and then the order domain analysis can be obtained by FFT transformation in the angle domain.

The fault characteristic frequency can be calculated for accurate fault location to diagnose the specific fault type of a long-used and damaged bearing [18]. However, for the variable speed, the fluctuating speed may cause the 'smearing problem' in the frequency domain, namely, multiple defect frequency components. To solve this dense problem, order analysis is carried out with resample techniques in order domain [19].

Firstly, the periodic revolution signal of shaft $V(w)$ can be defined as follows:

$$V(w) = sin((\sum_{s=1}^{w} \frac{v(s) \cdot 2\pi}{60} / f_s)), w = 1, ..., \Omega \tag{1}$$

Where $v(s)$ is the speed (rpm) collected from the tachometer. f_s is the sampling rate.

Then, the immediate phase of the periodic shaft revolution signal $\phi_{inst}(w)$ can be obtained:

$$\phi_{inst}(w) = arctan \frac{H[V(w)]}{V(w)} \tag{2}$$

Where H represents the discrete Hilbert transform [20], a type of discrete envelope method.

Subsequently, angle increment ϖ can be calculated:

$$\varpi = \frac{2\pi}{f_{shaft}} \tag{3}$$

Finally, the de-noising processing signal can be reconstructed or resampled within brand-new order domain, and the order domain is represented as follows:

$$\begin{aligned} O_{inner} &= \frac{N_b}{2} \cdot (1 + \frac{d_b}{d_p} cos\alpha)/R_r \\ O_{outer} &= \frac{N_b}{2} \cdot (1 - \frac{d_b}{d_p} cos\alpha)/R_r \\ O_{ball} &= \frac{d_p}{2d_b} \cdot (1 - (\frac{d_b}{d_p} cos\alpha)^2)/R_r \end{aligned} \tag{4}$$

Where O_{outer}, O_{inner} and O_{ball} indicate the fault characteristic order (FCO) of inner race, outer race and balls respectively. d_b and d_p are diameter of ball and pitch respectively. α is bearing contact angle. R_r is gear ratio, proportional to the bearing speed.

3. The proposed method

Our method for the diagnosis of wind turbine blade bearings consists of two parts: signal filter and fault inference. The signal filter is divided into 'model construction' and 'sparse model estimation' with 'coarse search' and 'fine search'. After signal filter, the denoised signal proceeds to fault inference to obtain the results of fault diagnosis. If the rotation speed of the wind turbine blade bearings is fixed speed, the 'frequency analysis' is carried out, while 'order analysis' is executed if it is variable speed. The whole framework of our method is shown in Fig. 1.

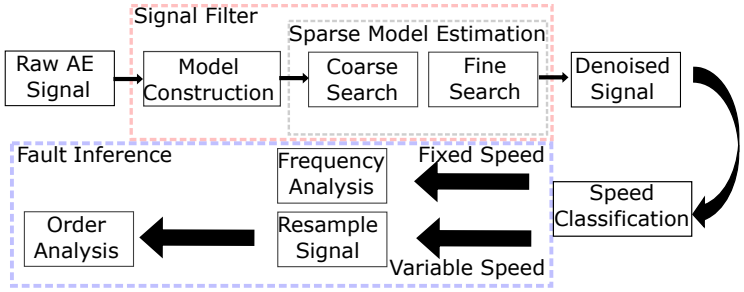

Figure 1: The complete flow chart for fault diagnosis.

3.1. Model Construction

The raw acoustic emission (AE) signal collected from industrial wind turbine blade bearings consists of two components: deterministic signals and fault signals [21, 22]. The deterministic signals are often undesired signals, such as mechanical rotation movements and electric signals, that must be eliminated. As for the fault signals generated due to damaged components, they are useful for further analysis and must be separated from the raw AE signals. In other words, the raw wind turbine blade bearing signal can be represented with the addition of two components, as shown in (5):

$$y(n) = d(n) + \xi(n), \quad n = 1, ..., M + N \tag{5}$$

Where $y(n)$ is the raw bearing signal, $d(n)$ and $\xi(n)$ represent deterministic signal and fault signal, respectively. The notations M and N are related to the dimensional size of the designed dictionary matrix, which is the key for our algorithms and will be explained in the following context. The deterministic component can be constructed based on a period of historical recordings [23], with both linearity and non-linearity terms [24]:

$$\begin{aligned}\hat{d}(n) &= \sum_{i_1=1}^{M} y(n-i_1)\theta_{i_1} + \sum_{i_2=1}^{M} y(n-i_2)^2\theta_{i_2} + ... \\ &+ \sum_{i_\gamma=1}^{M} y(n-i_\gamma)^\gamma\theta_{i_\gamma} \\ &= \sum_{j=1}^{\gamma}\sum_{i_j=1}^{M} y(n-i_j)^j\theta_{i_j}\end{aligned} \tag{6}$$

Where γ represents the nonlinear order index (NOI). The first term $\sum_{i_1=1}^{M} y(n-i_1)\theta_{i_1}$ in (6) is the linear component, and the $\sum_{i_1=1}^{M}\sum_{i_2=i_1}^{M}...\sum_{i_\gamma=i_{\gamma-1}}^{M}\prod_{v=1}^{\gamma} y(n-i_v)\theta_{i_1,...,i_v}$ means the γth order nonlinear component. The form of (6) is not intuitive and need to be reorganized, so the dictionary matrix P can be introduced and defined as follows:

$$P = \begin{bmatrix}\rho_1 & \rho_2 & ... & \rho_\gamma\end{bmatrix} \tag{7}$$

For each ρ_i in the matrix, both element possesses the dimension of $N \times M$, so the dimension of P is $N \times \gamma M$ where ρ_γ is detailed below:

$$\rho_\gamma = \begin{bmatrix} y(M)^\gamma & y(M)^{\gamma-1}y(M-1) & ... & y(1)^\gamma \\ y(M+1)^\gamma & y(M+1)^{\gamma-1}y(M) & ... & y(2)^\gamma \\ \vdots & \vdots & \vdots & \vdots \\ y(M+N-1)^\gamma & y(M+N-1)^{\gamma-1}y(M+N-2) & ... & y(N)^\gamma \end{bmatrix} \tag{8}$$

Subsequently, the formula (6) can be represented in matrix form:

$$\hat{D} = P\Theta \tag{9}$$

Where $\hat{D} = [\hat{d}(M+1), \hat{d}(M+2), ..., \hat{d}(M+N)]^T$ and $\Theta = [\theta_1, \theta_2, ..., \theta_{\gamma M}]^T$

So, the formula (5) can also be rewritten as the matrix format as:

$$Y = P\Theta + \Xi \tag{10}$$

Where $Y = [y(M+1), y(M+2), ..., y(M+N)]^T$ and $\Xi = [\xi(M+1), \xi(M+2), ..., \xi(M+N)]^T$

3.2. Bayesian and Adapted Kalman Augmented Lagrangian (BAKAL) Algorithm

BAKAL is proposed as a model optimization method that consists of two parts (coarse search and fine search) and can improve the fault diagnosis performance for wind turbine blade bearings. The dictionary matrix P shown in (7) contains all linearity and non-linearity terms which are usually redundant for deterministic signals $\hat{D}$ and this redundant information always results in difficult convergence during model construction, especially for the complex series data. So, the preliminary 'Coarse Search' will eliminate the most useless terms in our models and determine the rough model parameters. Afterwards, the parameters will be smoothed and modulated again on 'Fine Search' to denoise the raw AE signal.

B1. Coarse Search — Based on Bayesian Method

In order to deal with the time-varying condition, the sliding window concept is applied for raw AE signals. If the window length is L_w, the sliding length for each movement is L_s, the raw AE signal length is L_r, define W:

$$W = [w_1, w_2, ..., w_i] \tag{11}$$

Where the index of last element i is $(L_r - L_w)/L_s$.

Each window w_i is an independent state, approximate Hidden Markov Model (HMM). It can be first assumed that the current window only depends on the previous window. Then if the suitable window length is adopted, each window will be relatively dependent because the raw AE signal always conforms to a specific period. The two assumptions above are both valid conditions of HMM.

Then, according to [25], for each window w_i, fitting the equation $Y = P\Theta$ can be solved as the l_1-*norm* minimization problem described as follows:

$$\hat{\Theta}_{k+1} = \arg\min_{\theta} \frac{1}{2} \left\{ \left\| P\Theta - Y \right\|_2^2 + \lambda \left\| G\Theta \right\|_1 \right\} \tag{12}$$

Where $\hat{\Theta}_{k+1}$ is the adjusted parameter in the kth iteration. $\lambda \in (0, 1)$ is the hyper-parameter related to penalty to avoid over-fitting. G is a diagonal matrix, which directly influences each iteration, and the G in the kth iteration can be represented as follows:

$$G_k = diag[P^T(\lambda I + P\Gamma_k P^T)^{-1}P)]^{\frac{1}{2}} \tag{13}$$

Where $\Gamma_k = diag[\hat{\gamma}_k]$, and $\hat{\gamma}_k = |(\hat{\Theta}_k)|./(G_{k-1})$. I means the identity matrix.

Furthermore, the formula (12) can be represented as a quadratic optimization:

$$\min_{\theta, v \epsilon R^M} f_1(\Theta) + f_2(v) + \frac{\mu}{2} \left\| G\Theta - v \right\|_2^2 \tag{14}$$

Where $f_1(\Theta) = \frac{1}{2} \left\| P\Theta - Y \right\|_2^2, f_2(v) = \lambda \left\| v \right\|_1$. μ is Lagrange multiplier, which helps to drive the solution of (14) to be close to the weighted l_1-*norm* minimization problem (12).

According to the theorem of the augmented Lagrangian idea, the optimization problem can be further represented as unconstrained format [25, 26]:

$$\begin{aligned} L_\mu(\Theta, v, u) =& f_1(\Theta) + f_2(v) - u^T(G\Theta - v) \\ &+ \frac{\mu}{2} \left\| G\Theta - v \right\|_2^2 \end{aligned} \tag{15}$$

Where u indicates a dual variable. Replacing u with the variable $d = u/\mu$, we can obtain:

$$\begin{aligned} L_\mu(\Theta, v, d) =& f_1(\Theta) + f_2(v) \\ &+ \frac{\mu}{2} \left\| G\Theta - v - d \right\|_2^2 \end{aligned} \tag{16}$$

Then, quadratic optimization (14) is solved by processing the following three sub-problems, separately:

$$\hat{\Theta}_{k+1} = \arg\min_{\Theta} f_1(\Theta) + \frac{\mu}{2} \left\| G\Theta - v_k - d_k \right\|_2^2 \tag{17}$$

$$v_{k+1} = \arg\min_{v} f_2(v) + \frac{\mu}{2} \left\| G\hat{\Theta}_{k+1} - v - d_k \right\|_2^2 \tag{18}$$

$$d_{k+1} = d_k - (G\hat{\Theta}_{k+1} - v_{k+1}) \tag{19}$$

It is worth pointing out that the more proper regularization parameter results in a better model performance. Therefore, the regularization parameter λ will be adjusted according to the previous model iteration error during the iterated process.

Define model iteration error at $k+1$ iteration as:

$$\varepsilon_{k+1} = \left\| P\hat{\Theta}_{k+1} - Y \right\|_2^2 \tag{20}$$

Then the process can be summarized as follows, $c \in (0,1)$:

$$\lambda_{k+1} = \begin{cases} a\lambda_k, (a>1) & if \quad |\frac{\varepsilon_{k+1}}{\varepsilon_k} - 1| < c \\ b\lambda_k, (0<b<1) & if \quad |\frac{\varepsilon_{k+1}}{\varepsilon_k} - 1| \geq c \end{cases} \tag{21}$$

The general steps for the coarse search can be outlined as pseudo code form as follows:

Algorithm 1 Coarse Search

Initialization:
$k = 0, c \in (0,1), \lambda_0 = \mu \in (0,1), v_0 = d_0 = 0, G_0 = I$
while $sign(\hat{\Theta}_{k+1}) = sign(\hat{\Theta}_k); |\hat{\Theta}_{k+1}| - |\hat{\Theta}_k| \to 0$ **do**
  $\hat{\Theta}_{k+1} = (P^T P + \mu G_k^T G_k)^{-1}(P^T Y + \mu G_k^T (v_k + d_k))$
  $v_{k+1} = max(0, (G_k\hat{\Theta}_{k+1} - d_k)$
  $-\mu/\lambda_k) - max(0, -(G_k\hat{\Theta}_{K+1} - d_k) - \mu/\lambda_k)$
  $d_{k+1} = d_k - (G_k\hat{\Theta}_{k+1} - v_{k+1})$
  $G_{k+1} =$
  $diag[P^T(\lambda_k I + P(diag[|(\hat{\Theta}_{k+1})|./(G_k)])P^T)^{-1}P]^{\frac{1}{2}}$
  $\varepsilon_{k+1} = \left\| P\hat{\Theta}_{k+1} - Y \right\|_2^2$
  $\lambda_{k+1} = \begin{cases} a\lambda_k, (a>1) & if \quad |\frac{\varepsilon_{k+1}}{\varepsilon_k} - 1| < c \\ b\lambda_k, (0<b<1) & if \quad |\frac{\varepsilon_{k+1}}{\varepsilon_k} - 1| \geq c \end{cases}$
  $k = k + 1$
end while

Remark: During the iterations, the Θ_{k+1} can be pruned to obtain zero coefficients, when Θ_{k+1} is small enough.

B2. Fine Search — Based on Kalman Method

Assume we have a sequence of unobserved windows $w_1, w_2, ..., w_i$. For each unobserved window, we have $\Theta_{w_1}, \Theta_{w_2}, ..., \Theta_{w_i}$, with corresponding observation $z_{w_1}, z_{w_2}, ..., z_{w_i}$ [27, 28]. With regard to wind turbine blade bearings, the Θ_{w_i} denotes the model parameters in the ith window, and the z_{w_i} indicates the expected model parameters in the ith window.

The action-transition equation can be represented as:

$$\Theta_{w_k} = F_k\Theta_{w_{k-1}} + B_k u_k + \tau_k \tag{22}$$

The term $B_k = 0$, because this paper considers no input (u_k) system (my algorithm is also applicable for systems that have input). The real action-transition equation can be simplified as:

$$\Theta_{w_k} = F_k\Theta_{w_{k-1}} + \tau_k \tag{23}$$

Where F_k and B_k are state transfer matrix and control matrix respectively. u_k is control input. τ_k is process noise, with mean value zero, $\tau_k \sim N(0, Q_k)$.

The observation equation can be expressed as:

$$z_{w_k} = H_k\Theta_{w_k} + \eta_k \tag{24}$$

Where H_k is observation matrix. η_k is observation noise, with mean value zero, $\eta_k \sim N(0, R_k)$.

Define C is the covariance of posterior estimation error. $\hat{\Theta}$ is the estimated value. S_k is the covariance of measurement residual. K is Kalman gain. F_k and H_k are state transfer matrix and observation matrix respectively, which are both recommended as 1 in this case to reduce complexity, and the last search or adjustment process is shown below:

Algorithm 2 Fine Search

Prediction:
$\hat{\Theta}_{w_{k|k-1}} = F_k \hat{\Theta}_{w_{k-1|k-1}}$
$C_{k|k-1} = F_k C_{k-1|k-1} F_k^T + Q_k$
Update:
$\hat{z}_{w_k} = \frac{1}{k} \sum_{i=w_i-k}^{w_i} \Theta_i$
$\hat{m}_k = \hat{z}_{w_k} - H_k \hat{\Theta}_{w_{k|k-1}}$
$S_k = H_k C_{k|k-1} H_k^T + R_k$
$K_k = C_{k|k-1} H_k^T + (S_k)^{-1}$
$\hat{\Theta}_{w_{k|k}} = \hat{\Theta}_{w_{k|k-1}} + K_k \hat{m}_k$
$C_{k|k} = (I - K_k H_k) C_{k|k-1}$

Remark: $\hat{z}_{w_k}$ is the expected value according to last k Θ, and is able to adjust automatically to obtain better searching results.

Finally, if the optimal Θ is determined, the denoised signal can also be obtained through the following formula:

$$X_d = sign(X)|X - \Delta \hat{\Theta}_k| \tag{25}$$

The work flowchart for the BAKAL denoising process is shown in Fig. 2. The raw signal is first processed by sliding windows, and then the dictionary matrix is obtained according to these windows. Subsequently, the coarse search and fine search can help find the optimal model parameters. Finally, combined with the raw signal matrix, the signal can be denoised and output.

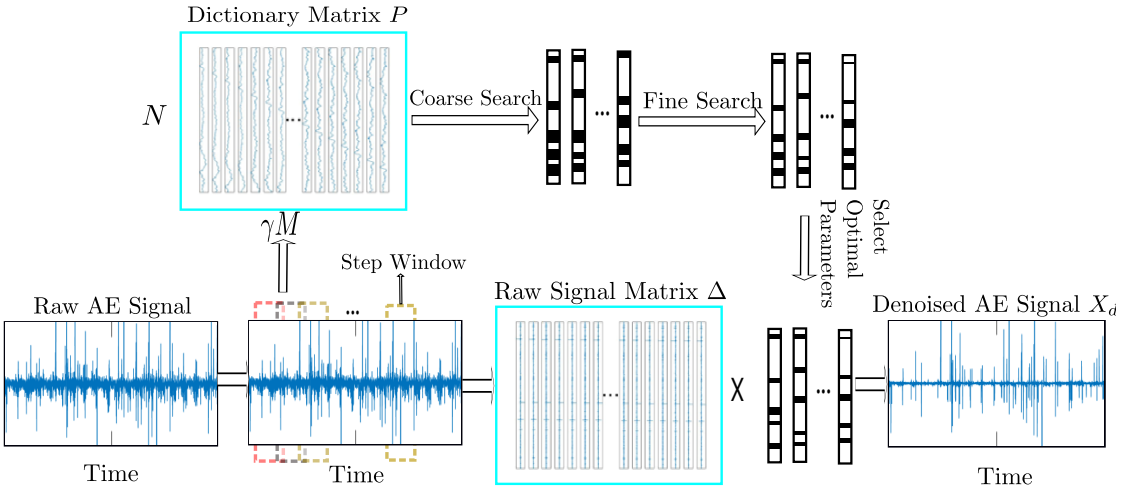

Figure 2: BAKAL denosing process.

4. Experiments and Results

The industrial-scale wind turbine blade bearing for experiments in this paper is 261 kg with a pitch diameter of 1 m, which has operated in an actual industrial wind power plant for more than 15 years. Furthermore, unlike most research studies, our experiments in this paper do not use artificially damaged or small-scale wind turbine models but naturally formed damage during the service period. In order to approximate the actual maintenance situation, the industrial wind turbine is equipped with a 7.75 m and 139 kg loading (blade) on the blade bearing, as shown in Fig. 3.

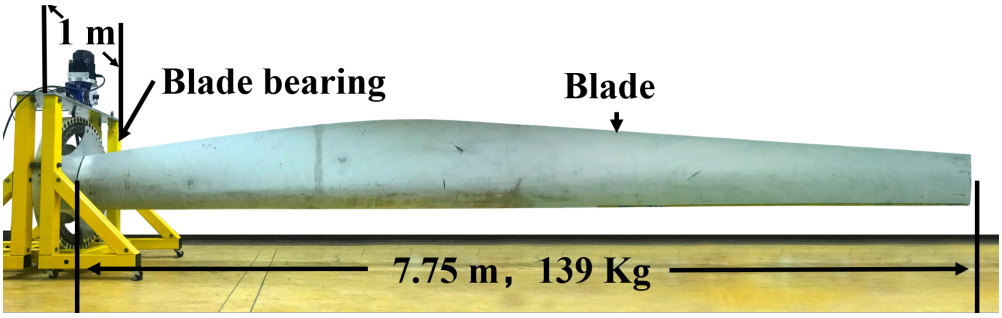

Figure 3: Front view of wind turbine blade bearing.

In order to diagnose the defect type, the bearing speed needs to be measured to determine the fault characteristic frequencies (FCF) for fault diagnosis. When the bearing is measured directly in a real industrial wind turbine, the flapping and trembling blades could add redundant disturbance to the bearing surface, making measurement difficult. So, considering convenience and flexibility, the gearbox shaft speeds are measured instead, using a tachometer, an equivalent indirect measurement based on the transmission ratio (gear ratio) between bearing speed v_b and gearbox shaft speed v_g. According to the gear ratio R_r ($R_r = 5.33$), the real bearing rotation of three tests can be calculated ($v_b = v_g/R_r$).

In order to validate the efficiency of our algorithm for fault diagnosis, three tests are conducted. They are Test 1 (approximately fixed speed with tiny fluctuations, without a blade, 2.16 ± 0.02 r/min), Test 2 (variable speed, with a blade, 1.63 r/min to 1.91 r/min) and Test 3 (variable speed, with a blade, 3.62 r/min to 3.81 r/min), respectively. Test 1 is executed with an approximately fixed gearbox shaft speed of 11.50 r/min. Test 2 and Test 3 are both variable gearbox shaft speeds, varying from 8.70 r/min to 10.20 r/min and 19.30 r/min to 20.30 r/min, respectively. Test 1 is a basic condition with negligible fluctuation of wind turbine blade bearing rotation speed. At the same time, Test 2 and Test 3 simulate complex conditions with relatively large fluctuation for the really fickle blade flipping and unsteady factors, occasionally resulting in some fluctuation. So, both fixed and variable speed tests are important and are carried out for comparison to further validate the efficiency of our algorithm.

The fault characteristic frequency (FCF) and fault characteristic order (FCO) are significant helpers in determining the fault type of wind turbine blade bearings. According to average bearing speed and inherent parameters, the theoretical fault characteristic frequencies can be calculated [9]. The calculated FCF is shown in Table 1.

Table 1: Theoretical FCF of the wind turbine blade bearing.

Test ID	Bearing Speed (r/min)	f_{inner} (Hz)	f_{outer} (Hz)	f_{ball} (Hz)
Test 1	2.16	1.1173	1.0424	0.3329
Test 2	1.63 - 1.91	0.9156	0.8542	0.2728
Test 3	3.62 - 3.81	1.9244	1.7953	0.5733

The theoretical FCO of this bearing can be obtained by formula (4), which is deterministic for this particular blade bearing, as shown in Table 2.

The raw AE signal consists of two main components: bearing fault signals (useful information generated through periodic bumping due to defects) and deterministic signals (undesired noise, such as mechanical rotation movement signals and electric signals). In order to make a more accurate analysis and avoid noise interference, the deterministic signals need to be filtered. Meanwhile, the fault signal should be retained as much as possible too. For the proposed BAKAL method, some tunable parameters have to be chosen, as

Table 2: Theoretical FCO of the wind turbine blade bearing.

R_r	O_{inner}	O_{outer}	O_{ball}
5.33	5.824	5.433	1.735

shown in (8).

The tunable parameter N, the length of input data for the sliding window, was tried with the following values: 100, 500, 1000, 2000, and 5000, and it was found that small N results in under-fitting performance and large N brings over-fitting performance, so the value 1000 was selected. For the parameter γ, large γ introduces more non-linearity terms and increased computation complexity, so it was set at 2, just guaranteeing inclusion of non-linearity. The parameter M is related to historical information that is referred by our model. A wide range of testing values 10, 40, 80, 160, and 640 are tried for M and it was found that the denoising performance will not be better after M is increased to 160, so the 160 was selected. After some trial and adjustment of tunable parameters, the model parameters for Test 1 are $N = 1000$, $\gamma = 2$ and $M = 160$. The tunable parameters for Test 2 and Test 3 are the same as Test 1, both $N = 1000$, $\gamma = 2$, and $M = 160$.

The kurtosis value has been widely used as an indicator to measure denoising performance [26]. The high kurtosis value often indicates that small amounts of noise exist in the signal. Meanwhile, we need to exclude a very high kurtosis value resulting from an over-fitting model that over eliminates useful fault information. In other words, the perfect denoised signal should have a large kurtosis under the premise of the valuable component being fully conserved. To verify that the valuable component is retained, the corresponding FCF or FCO should be calculated and inferred through the denoising signal. Through the BAKAL algorithm process, the kurtosis value of the signal reaches 2910.53, indicating good filtering performance, as shown in Fig.4(c).

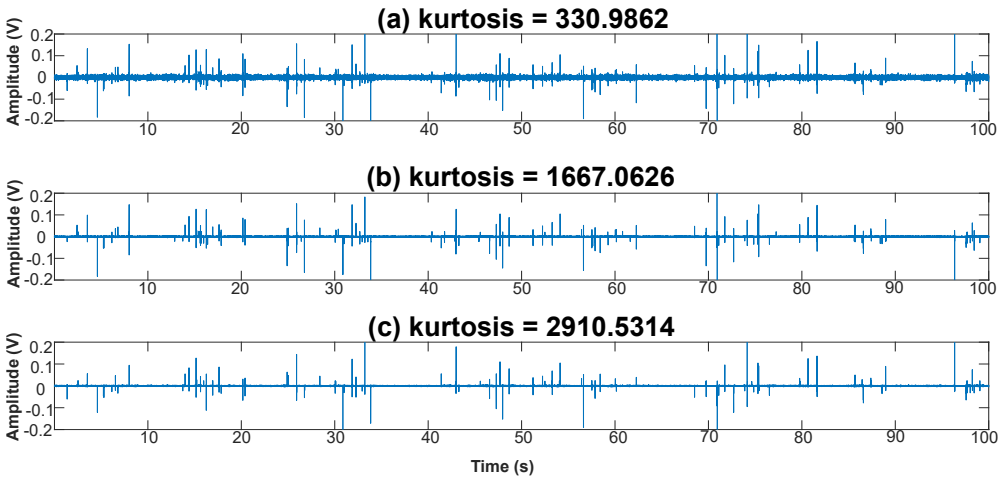

Figure 4: Test 1 results: (a) raw AE signal (b) BAL denoised signal (c) BAKAL denoised signal.

Fig.4(a) is the raw AE signals of Test 1 obtained from acoustic sensors directly. It is observed that the fault signals are heavily interfered by redundant noise, although the wind turbine blade bearing rotation speed of Test 1 is fixed. The kurtosis value of the raw AE signal for Test 1 is 330.99, and the kurtosis rises to 1667.06 after the BAL algorithm processing, as presented in Fig.4(b). Furthermore, denoising performance still has significant enhancement after using the BAKAL algorithm (kurtosis up to 2910.53), as indicated in Fig.4(c). According to the aforementioned analysis in the time domain, this may denote that the BAKAL method has better filtering performance than the BAL method.

To understand why the new method performs better, the model parameters Θ and their time-varying changes are shown in Fig.5 and Fig.6. As can be seen, the BAKAL method has smoother and less oscillation model parameters, leading to more robust filtering performance. The detailed explanation of Fig.5 and Fig.6 are shown respectively in the following text.

The total number of the model parameters Θ is 160, but all have similar performance and phenomena, so only one of them is selected to clarify the necessity of using the sliding window. Fig.5 shows the variation of a specific model parameter in different windows. As shown in Fig.5, severe fluctuations are existed for a specific model parameter among different step windows. For example, the model parameter value for window a is close to 0, but the corresponding value for window b and window c are around -10 and 14, respectively. This demonstrates that the differences among these windows are significant, indicating the time-varying nature of the raw AE signal.

The number of the windows is chosen as 2000, but all windows denote a similar phenomenon, so only one of them is chosen to emphasize the advantage of BAKAL compared with BAL. Fig.6 shows all the model parameter values from one specific window results for both BAKAL and BAL. BAKAL has much more smooth model parameter values with fewer oscillations for the nonlinear part than BAL, which is why BAKAL produces better filtering results than BAL. Meanwhile, both BAKAL and BAL can have sparse results since the first 80 parameter values for the linear part of the model are zero or near zero. This phenomenon also reflects that the noise is not linear but more nonlinear in nature.

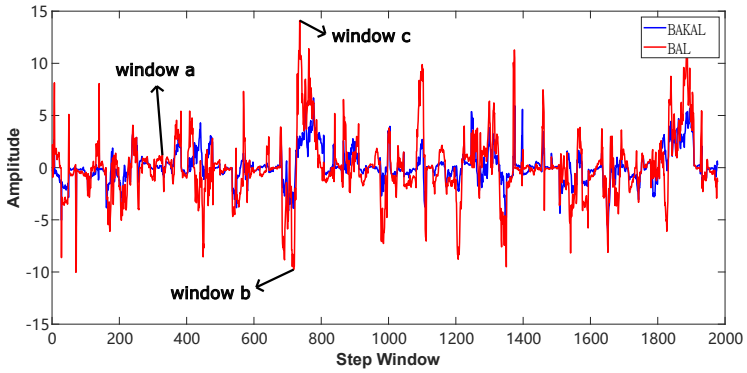

Figure 5: Observation of inner model parameter values from the perspective of a certain model parameter.

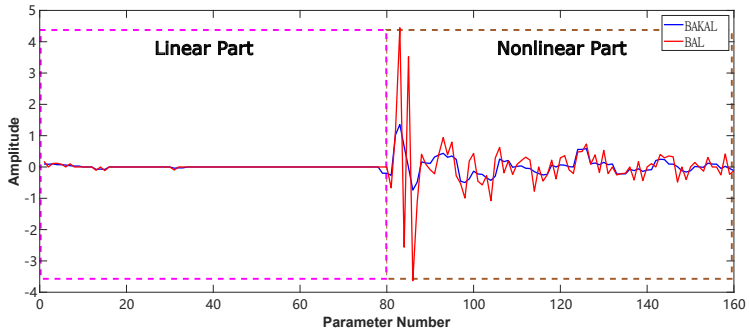

Figure 6: Observation of inner model parameter values from the perspective of a certain window.

After the preliminary noise reduction through the proposed BAKAL method, the analysis in frequency spectra brings more crucial information for bearing condition monitoring. To analyze whether the bearing has a fault, the spectrum of the fault envelop signal has to be calculated and then compared with the known theoretical FCF. The possible fault can be inferred if one abnormal frequency in frequency spectra is close to one of the theoretical FCFs. As shown in Fig.7, both the BAL processed and the BAKAL processed results

exist a unique point around frequency 1.1 Hz, with amplitude 7.649×10^{-5} and 1.051×10^{-4}, respectively. Then referring to $f_{inner} = 1.1173$ Hz in Table 1, this indicates that the inner race crack may exist. Although both the BAL and BAKAL method can recognize the correct fault frequency, the BAKAL method has higher amplitude point at theoretical FCF and lower amplitude points at non-theoretical FCF.

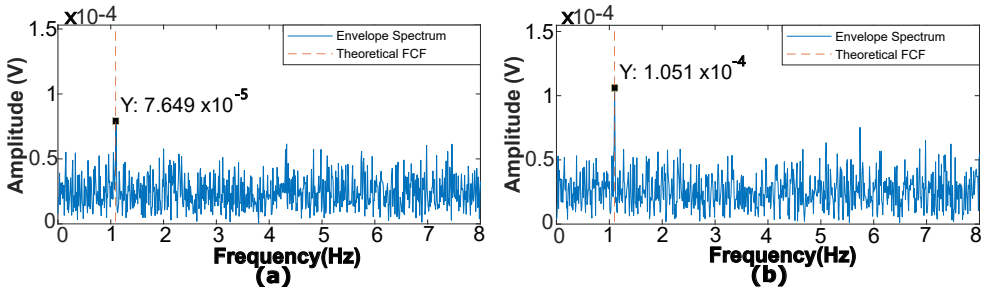

Figure 7: Hilbert transform based frequency spectrogram of Test 1: (a) BAL processed (b) BAKAL processed.

After the approximately fixed speed Test 1 is done, two variable speed tests (Test 2 and Test 3) are carried out to compare and validate the performance of the proposed method. As shown in Fig.8 and Fig.9, BAKAL processed signals in Test 2 and Test 3 both possess a larger kurtosis value than BAL processed. This may denote that the BAKAL method performs better than the BAL method in terms of filtering performance, which holds the same conclusion as that of Test 1. Fig.10 and Fig.11 also have similar regularity as Fig.5 and Fig.6, illustrating the time-varying nature of raw signal and smoothness characteristic of the BAKAL method. Then, Fig.12 (a) and Fig.12 (b) show the spectra of the envelop of the denoised signal for both tests. It can be seen that the highest amplitude for Test 2 and Test 3 exists in 0.96 Hz and 1.92 Hz, respectively. It is difficult to distinguish the highest amplitude from many high points nearby because of the 'smearing problem' due to the variable bearing rotated speed. In order to solve the 'smearing problem' in frequency spectra, the signal is resampled in the order domain to obtain the order spectrum further.

Fig.13 and Fig.14 demonstrates the order spectra of the denoised signals in Test 2 and Test 3, which are resampled in the order domain, respectively. Referring to the theoretical $O_{inner} = 5.824$, the BAKAL processed results Fig.13(b) and the Fig.14(b) can denote that the blade bearing fault for these two tests both occur in the inner race, which is also consistent with the actual damage to this bearing. Fig.13 (a) and Fig.14 (a) show the order domain spectra of the BAL method in Test 2 and Test 3. The identified FCO value is heavily contaminated and it is difficult to identify. In contrast with the corresponding spectra of BAKAL, namely Fig.13 (b) and Fig.14 (b), the BAKAL results in a more distinguishable point than BAL at theoretical FCO, so that we can clearly determine the corresponding fault. Summarizing the results of Fig.13 and Fig.14, the BAKAL may possess two advantages: 1) higher amplitude point at theoretical FCO. 2) lower amplitude points at non-theoretical FCO.

Overall, not only for the approximately fixed speed experiment (Test 1) but also for the variable speed experiment (Test 2 and Test 3), the new BAKAL algorithm performs better both in the time domain and frequency domain (or order domain), with better fault detection results due to its superior filtering performance.

5. Damage Validation

In order to validate the results of fault diagnosis, an electronic endoscope is utilized to inspect the industrial-scale wind turbine blade bearing (261 kg with pitch diameter 1 m, served for 15 years) in this paper. Fig.15 from endoscope shows that the defect (measured size: 9mm length and 5mm height) exists at the bearing inner race. Moreover, the endoscope can not detect other cracks on the bearing balls or the bearing outer race. This detection result confirms that the above diagnostic results are correct. Hence, the proposed BAKAL method in this paper can be helpful for fault diagnosis of wind turbine blade bearings, indicating the broad application prospect of our method for a natural industrial environment.

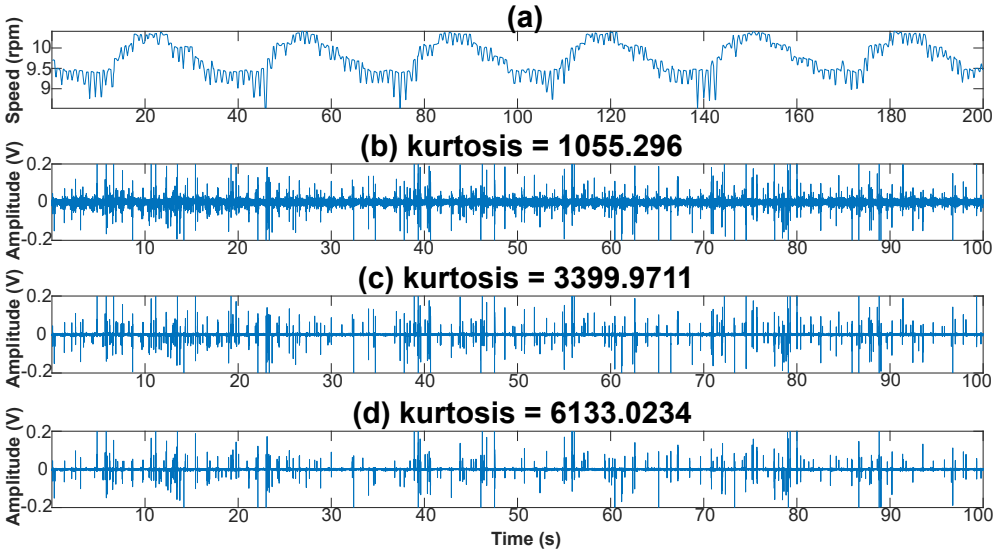

Figure 8: Test 2 results: (a) collected gearbox shaft speed (b) collected raw AE signal (c) BAL processed signal (d) BAKAL processed signal.

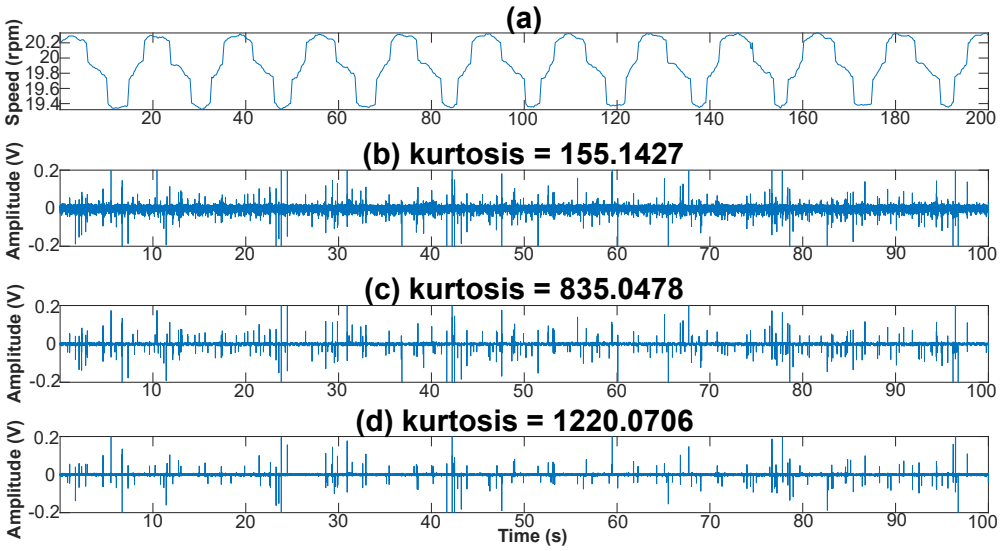

Figure 9: Test 3 results: (a) collected gearbox shaft speed (b) collected raw AE signal (c) BAL processed signal (d) BAKAL processed signal.

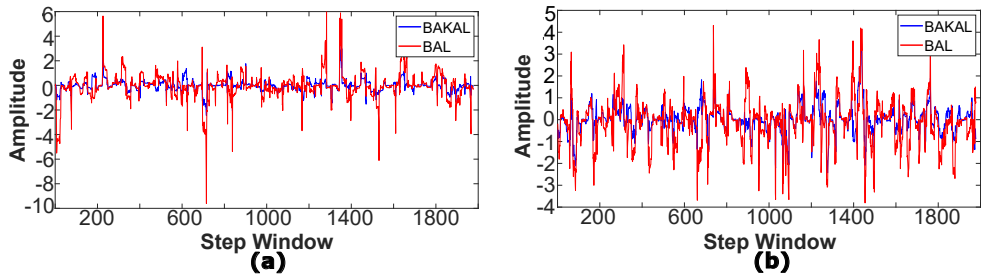

Figure 10: Observation of inner model parameter values from the perspective of a certain model parameter, (a) Test 2 and (b) Test 3.

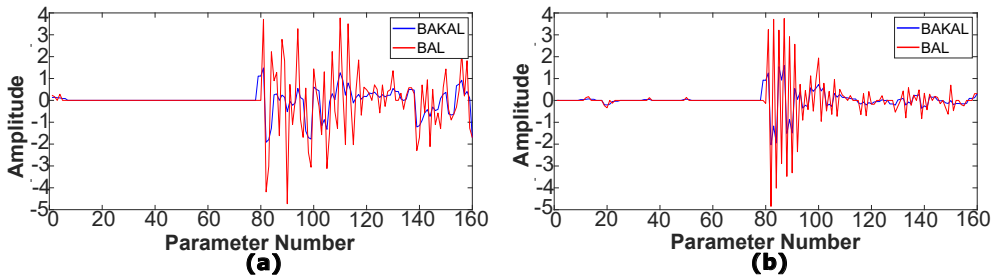

Figure 11: Observation of inner model parameter values from the perspective of a certain window, (a) Test 2 and (b) Test 3.

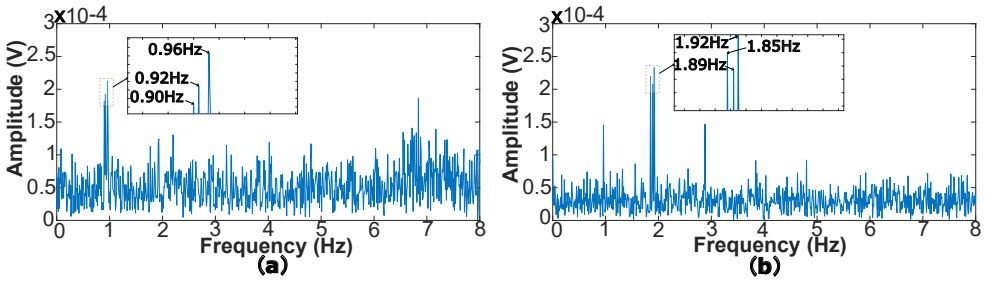

Figure 12: Hilbert transform based frequency spectrogram of (a) Test 2 and (b) Test 3.

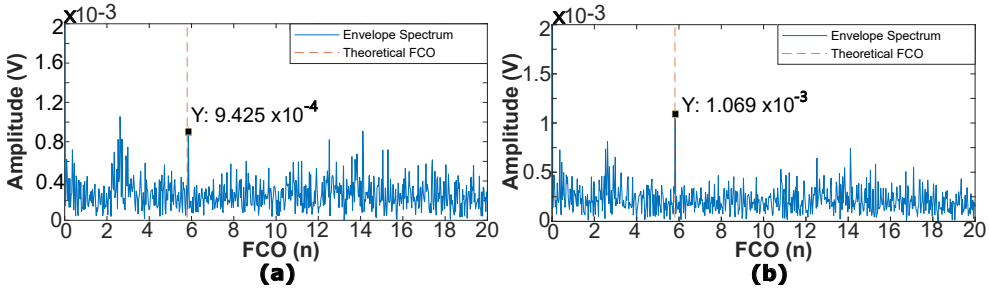

Figure 13: Hilbert transform based order spectrogram of Test 2: (a) BAL processed (b) BAKAL processed.

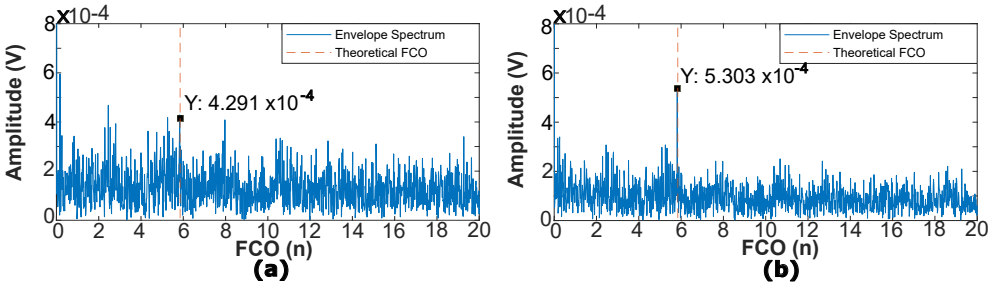

Figure 14: Hilbert transform based order spectrogram of Test 3: (a) BAL processed (b) BAKAL processed.

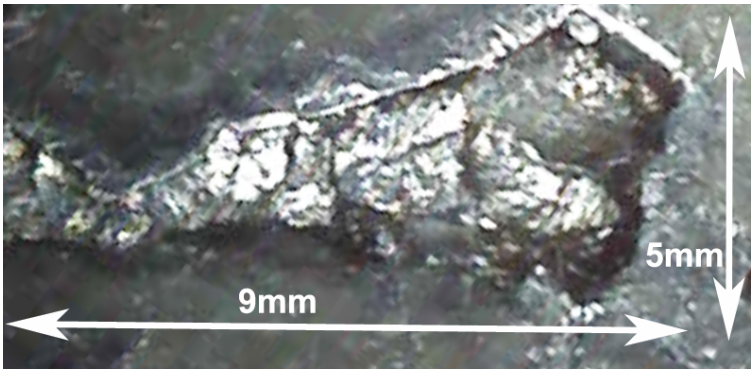

Figure 15: Inner race defect through endoscope.

6. Conclusion

This paper has proposed the Bayesian and Adapted Kalman Augmented Lagrangian (BAKAL) method, which is an extended and improved method from the Bayesian Augmented Lagrangian (BAL) [25], for fault detection of wind turbine blade bearings under the condition of fluctuating slow speed. The proposed BAKAL method provides two primary merits. Firstly, it can process the time-varying signal during the oscillation phase, but this problem needs to be simplified as a time-invariant system in BAL. Secondly, it improves the parameter optimization process with two steps (coarse search and fine search) to improve model parameter estimation during model construction, which results in more consistent parameters and better denoising performance. The experimental results of industrial-scale wind turbine blades illustrate that the BAKAL method can detect the fault of wind turbine blade bearing, and it is superior to the BAL method in terms of raw signal denoising. In addition, the BAKAL method is compatible with the BAL method, so the original merits (non-linearity and sparsity) of BAL are also conserved in BAKAL.

7. Acknowledgments

This work was supported in part by the RCUK under Grant (EP/ S017224/1)

References

[1] R. S. Amano, Review of wind turbine research in 21st century, Journal of Energy Resources Technology 139 (5).
[2] G. W. E. Council, Global wind report 2016–annual market update, Global Wind Energy Council: Brussels, Belgium.
[3] J. Wang, Y. Peng, W. Qiao, J. L. Hudgins, Bearing fault diagnosis of direct-drive wind turbines using multiscale filtering spectrum, IEEE Transactions on Industry Applications 53 (3) (2017) 3029–3038.
[4] S. Sheng, Report on wind turbine subsystem reliability-a survey of various databases (presentation), Tech. rep., National Renewable Energy Lab.(NREL), Golden, CO (United States) (2013).

[5] R. Liu, B. Yang, A. G. Hauptmann, Simultaneous bearing fault recognition and remaining useful life prediction using joint-loss convolutional neural network, IEEE Transactions on Industrial Informatics 16 (1) (2019) 87–96.
[6] X. Jin, Z. Que, Y. Sun, Y. Guo, W. Qiao, A data-driven approach for bearing fault prognostics, IEEE Transactions on Industry Applications 55 (4) (2019) 3394–3401.
[7] D. Mba, R. Rao, Development of acoustic emission technology for condition monitoring and diagnosis of rotating machines: bearings, pumps, gearboxes, engines, and rotating structures, Shock and Vibration Digest 38 (1) (2006) 3–18.
[8] Z. Liu, B. Yang, X. Wang, L. Zhang, Acoustic emission analysis for wind turbine blade bearing fault detection under time-varying low-speed and heavy blade load conditions, IEEE Transactions on Industry Applications 57 (3) (2021) 2791–2800.
[9] Z. Liu, X. Wang, L. Zhang, Fault diagnosis of industrial wind turbine blade bearing using acoustic emission analysis, IEEE Transactions on Instrumentation and Measurement 69 (9) (2020) 6630–6639.
[10] S. A. Aye, P. S. Heyns, C. J. Thiart, Fault detection of slow speed bearings using an integrated approach, IFAC-PapersOnLine 48 (3) (2015) 1779–1784.
[11] Y. Guo, Z. Zhao, R. Sun, X. Chen, Data-driven multiscale sparse representation for bearing fault diagnosis in wind turbine, Wind Energy 22 (4) (2019) 587–604.
[12] D. Zhang, Y. Fu, Z. Lin, Z. Gao, A reinforcement learning based fault diagnosis for autoregressive-moving-average model, in: IECON 2017-43rd Annual Conference of the IEEE Industrial Electronics Society, IEEE, 2017, pp. 7067–7072.
[13] M. Yuan, Y. Wu, L. Lin, Fault diagnosis and remaining useful life estimation of aero engine using lstm neural network, in: 2016 IEEE international conference on aircraft utility systems (AUS), IEEE, 2016, pp. 135–140.
[14] Z. Liu, X. Tang, X. Wang, J. E. Mugica, L. Zhang, Wind turbine blade bearing fault diagnosis under fluctuating speed operations via bayesian augmented lagrangian analysis, IEEE Transactions on Industrial Informatics 17 (7) (2020) 4613–4623.
[15] P. Borghesani, P. Pennacchi, R. Randall, R. Ricci, Order tracking for discrete-random separation in variable speed conditions, Mechanical Systems and Signal Processing 30 (2012) 1–22.
[16] W. Huang, Z. Song, C. Zhang, J. Wang, J. Shi, X. Jiang, Z. Zhu, Multi-source fidelity sparse representation via convex optimization for gearbox compound fault diagnosis, Journal of Sound and Vibration 496 (2021) 115879.
[17] B. Yang, R. Liu, X. Chen, Fault diagnosis for a wind turbine generator bearing via sparse representation and shift-invariant k-svd, IEEE Transactions on Industrial Informatics 13 (3) (2017) 1321–1331.
[18] W. Huang, G. Gao, N. Li, X. Jiang, Z. Zhu, Time-frequency squeezing and generalized demodulation combined for variable speed bearing fault diagnosis, IEEE Transactions on Instrumentation and Measurement 68 (8) (2018) 2819–2829.
[19] F. Bonnardot, M. El Badaoui, R. Randall, J. Daniere, F. Guillet, Use of the acceleration signal of a gearbox in order to perform angular resampling (with limited speed fluctuation), Mechanical Systems and Signal Processing 19 (4) (2005) 766–785.
[20] L. Marple, Computing the discrete-time" analytic" signal via fft, IEEE Transactions on signal processing 47 (9) (1999) 2600–2603.
[21] J. Antoni, R. Randall, Unsupervised noise cancellation for vibration signals: part i—evaluation of adaptive algorithms, Mechanical Systems and Signal Processing 18 (1) (2004) 89–101.
[22] J. Antoni, R. Randall, Unsupervised noise cancellation for vibration signals: part ii—a novel frequency-domain algorithm, Mechanical Systems and Signal Processing 18 (1) (2004) 103–117.
[23] Z. Liu, L. Zhang, Naturally damaged wind turbine blade bearing fault detection using novel iterative nonlinear filter and morphological analysis, IEEE Transactions on Industrial Electronics 67 (10) (2019) 8713–8722.
[24] R. Huang, F. Xu, R. Chen, General expression for linear and nonlinear time series models, Frontiers of Mechanical Engineering in China 4 (1) (2009) 15–24.
[25] X. Tang, L. Zhang, X. Li, Bayesian augmented lagrangian algorithm for system identification, Systems & Control Letters 120 (2018) 9–16.
[26] J. Wang, W. Qiao, L. Qu, Wind turbine bearing fault diagnosis based on sparse representation of condition monitoring signals, IEEE Transactions on Industry Applications 55 (2) (2018) 1844–1852.
[27] R. E. Kalman, A new approach to linear filtering and prediction problems.
[28] D. P. Kingma, M. Welling, Auto-encoding variational bayes, arXiv preprint arXiv:1312.6114.